Sensors & Transducers, Vol. 181, Issue 10, October 2014, pp. 200-209

www.sensorsportal.com

Sensors & Transducers

http://www.sensorsportal.com

Optimization and Experimental Research of Combustion of Direct-injection Diesel Engine

[1, 2] Guanqiang Ruan, [1] Zhendong Zhang, [2] Jinrun Cheng
[1] University of Shanghai for Science and Technology,
No. 516, Jungong Road, Shanghai, 200093, China
[2] Shanghai Dianji University, No. 88, Wenjing Road, Shanghai, 200245, China
[1] Tel.: +86-021-64306661
E-mail: ruangq@sdju.edu.cn

Received: 7 July 2014 /Accepted: 30 September 2014 /Published: 31 October 2014

Abstract: Diesel Engine has got an increasingly wide utilization in engineering applications due to its thermal efficiency. Since there are some flaws on design of original engine, the emission performance of diesel engine is poor. In order to improve the performance of the diesel engine, the fuel injection advance angle of original engine is optimized, and a new advance angle of fuel injection is proposed in this paper. By numerical calculation with simulation of software FIRE, the effect of different combustion chamber structures on the cylinder pressure, temperature, accumulated heat release and the parameters such as NO_x mass fraction was analyzed. From the simulation results, the optimized fuel injection advance angle had greatly improved the diesel combustion and emission performance. Finally, via experimental verification, the engine with optimized fuel injection advance angle gets better dynamic performance, as well as less emission than original machine.

Keywords: Diesel engine, Combustion analysis, Parameter optimization, Experimental research.

1. Introduction

Energy saving and emissions reduction are eternal topics to automobile industry, with the international oil prices rising and the environmental deterioration due to the increased car ownership. To solve the above problem, a lot of countries in the world are actively looking for a solution. Because of the high thermal efficiency of the diesel engine, and with advantages of good power performance, low consumption, diesel engines have been widely used on passenger cars and trucks, diesel is a preferred solution instead of gasoline engine to relieve the energy crisis. But to get the higher thermal efficiency of diesel engine, combustion temperature in cylinder is higher, as well as the maximum explosion pressure. In the process of combustion, in addition to produce complete combusted emissions, a series of environmental pollutants are produced as well [1-5].

It is well known that, the three elements of NO_x generation are oxygen enrichment, high temperature and its duration, and high temperature, oxygen-poor to soot. Therefore, firstly it can reduce NO_x emission by controlling the amount of premixed combustion to reduce initial burning temperature, and then keep rapid combustion and high combustion temperature, reduce the diffusion combustion and make whole combustion duration shortened to reduce the PM emission and improve fuel economy. General Diesel engine combustion zone is crossing inevitably with generation area of carbon particles and NO_x, so it should try to move the combustion area to the low

NO_x and PM area to make all combustion carried out with lean gas mixture and low combustion temperature. But for the traditional diesel engine, it is impossible to completely realize the aforementioned combustion mechanism, so the generation of NO_x and PM is inevitable [6-8]. According to the guiding ideology of reducing the emissions, based on the generating mechanism of harmful emissions, maximally limit the generation of harmful emissions in the combustion chamber, fundamentally to reduce exhaust pollutant generation. For diesel engine, it can take various modified design methods to improve the emission performance based on the structure of the injection system and combustion chamber [9, 10].

In this context, it is of important theoretical significance and practical value to improve the environment pollution and postpone the energy crisis, by taking effective measures to reduce the harmful gas generation and emission of diesel engine [11]. By considering diesel engine combustion as the research object, this paper had established a numerical model of combustion procedure of diesel engine by means of CFD simulation, studied the influence of different parameters on the combustion performance and optimized the structural parameters of diesel engine. These improved the power performance and fuel economy, as well as reduced emissions effectively.

2. Model Establishment

Establishing an accurate mathematical model is the foundation and premise of a further study of diesel engine combustion process and the dynamic characteristics. In 1974, E. V. Bracco put forward that the combustion model can be divided into zero-dimensional model, the quasi-dimensional model and multi-dimensional model according to the dimensionality [12, 13]. Zero-dimensional model has been widely used in the design and research of internal combustion engine, there are various zero-dimension models in public reports, Wiebe model and Watson model are commonly used [14]. But in zero-dimension model, the working substance in cylinder is assumed to be uniformly distributed, it cannot describe the influence of significant physical processes such as spray, oil droplets evaporation, mixing, entrainment and working substance movement as well as the non-uniformed temperature field on harmful emissions, cannot be used for concentration prediction of harmful waste gas, also cannot analyze effects of spray, evaporation, mixing and flame propagation on combustion process. The combustion chamber is divided artificially into several regions, in each region, equations remain ordinary differential with time as the only variable, in turn, influence each other, and this kind of model is called the quasi-dimensional model. The original multi-dimensional numerical simulation can be traced back to the early 70s of last century, in the doctoral dissertation of Watkins, a two-dimensional axisymmetric gas flow particles in cylinder with no combustion and no injection are calculated [15]; Boni and Hirt et al. developed arbitrary Lagrange-Euler method with the combustion and turbulence model joined, two-dimensional model was used to analyze and simulate the engine's compression stroke and power stroke. Although these early simulations now look some rough, but it is them that laid a solid foundation for the numerical simulation development of diesel engine working process. Subsequently, in 1984 Gosman published his paper that solves the three-dimensional turbulent flow field in cylinder, multidimensional numerical simulation of internal combustion engine has entered a new stage of development [16].

2.1. Turbulence Model

From the perspective of the engineering CFD calculation, $k-\varepsilon$ model is a widely applied turbulence model currently, heat transfer and combustion flow can be calculated. The $k-\varepsilon$ model can generate real result relatively in the condition of a variety of characteristics, and mainly contains the transport equation of turbulent kinetic energy k and consumption rate ε [17].

$$\rho\frac{Dk}{Dt} \equiv \underbrace{\rho\frac{\partial k}{\partial t}}_{L} + \underbrace{\rho U_j \frac{\partial k}{\partial x_j}}_{C} = \underbrace{\rho \overline{f_i u_i}}_{\rho G} - \underbrace{\rho \overline{u_i u_j} \frac{\partial U_i}{\partial x_j}}_{\rho P} \\ \underbrace{-\mu \overline{\left(\frac{\partial u_i}{\partial x_j}\right)^2}}_{\rho\varepsilon} + \underbrace{\frac{\partial}{\partial x_j}\left(\mu\frac{\partial k}{\partial x_j} - \rho\overline{ku_j} - \overline{pu_i}\delta_{ij}\right)}_{D}, \quad (1)$$

where $\rho\frac{Dk}{Dt}$ is the turbulent kinetic energy, the subscript annotation L is for local variation, C is the amount of convection, D is the diffusion item, P and G are related to $\rho\frac{Dk}{Dt}$.

2.2. Spray Model

Basically the spray simulation uses Discrete Droplet Model (DDM).

The function to describe spray droplets is $f\left(x_i, u_{id}, m_d, D_d, T, t\right)$, differential form of conservation equation for droplets amount density is spray equation [18]:

$$\frac{\partial f}{\partial t} + \nabla x_i\left(f\cdot u_{id}\right) + \nabla u_{id}\left(f\cdot\alpha_i\right) + \frac{\partial}{\partial D_d}\left(f\cdot D_d\right) \\ + \frac{\partial}{\partial T}\left(f\cdot\frac{dT}{dt}\right) + \frac{\partial}{\partial m_d}\left(f\cdot\frac{dm_d}{dt}\right) = \frac{d}{dt}f_s, \quad (2)$$

where $\alpha_i = du_{id}/dt$ is the mass force of the unit. The expression is:

$$f_s = f_{inj} + f_{\alpha to} + f_b + f_{col} + f_{imp} + f \ , \quad (3)$$

Droplets flow equation is as follows:

$$m_d \frac{du_{id}}{dt} = F_{idr} + F_{ig} + F_{ig} + F_{ib} \, , \quad (4)$$

where $u_{id} = dx_{id}/dt$ indicates the droplets movement tracks; F_{idr} indicates resistance on droplets; F_{ig} indicates the joint action of gravity and buoyancy; F_{ig} indicates the pressure on droplets; F_{id} indicates the virtual mass force.

2.3. Flamelet Model

In combustion Model, this paper adopts ECFM-3Z Coherent Flamelet Model, which is put forward by F. E. Maeble and J. E. Broawell in 1977 [19], ECFM-3Z Model is very suitable for simulation of the diesel engine combustion, because there are premixed combustion and diffusion combustion in diesel engine, mainly diffusion combustion that can promote combustion. In ECFM-3Z, a turbulent mixing model is used to describe the mixing between fuel vapor and air in cylinder. The Mixing Model Parameter in ECFM-3Z model can influence the diffusion velocity of fuel and air to mixing area, the mixing of fuel and air becomes quicker with the increasing of this parameter to promote combustion. Because the ignition model comes with the ECFM-3Z model, there's no need to select an ignition model.

2.4. NO_x Emission Model

NO_x generation has a close relationship with air-fuel ratio, generally the NO_x generation concentrated on ϕ_a =1.1, and at this moment the OH concentration is very low, so the third equation generally can be ignored [20].

As aforementioned analysis, most of NO_x generates after mixture combustion has completed, so NO_x generation and combustion procedure can be processed separately. Local chemical equilibrium method is used to calculate thermal NO_x production, its expression is:

$$k_1[N_2]\cdot[O] = k_2[NO]\cdot[N], \quad (5)$$

$$k_3[N]\cdot[O_2] = k_4[NO]\cdot[O], \quad (6)$$

They can be simplified to:

$$N_2 + O_2 = 2NO, \quad (7)$$

According to the Zeldovich mechanism, the equation of NO_x generation rate is:

$$\frac{d[NO]}{dt} = 2k_f[N_2][O_2], \quad (8)$$

where $k_f = k_1 \cdot k_3$ is the positive reactive rate, $k_b = k_2 \cdot k_4$ is the reverse reactive rate.

$$k_f = \frac{A}{\sqrt{T}} \cdot \exp\left(-\frac{E_a}{RT}\right), \quad (9)$$

where A represents preexponential factor, E_a indicates activation energy.

2.5. Soot Emission Model

Generated rate of pure soot in cylinder is composed of generation rate and the oxidation rate [21]:

$$S_{\phi_S} = S_n + S_g + S_{O_2}, \quad (10)$$

where S_{ϕ_S}, S_n, S_g and S_{O_2} are the Pure soot source, crystal nucleus generation source, soot surface generation source and carbon oxide source respectively.

This article selects the Kennedy Hiroyasu Magnussen model as the soot generation and oxidation model, soot generation rate is calculated by the Khan-Hiroysau-Belardini formula, the generated source term of the soot surface:

$$S_g = A \cdot F(f, \varphi_S) \cdot p^{0.5} \cdot \exp\{-\frac{E_a}{R_T}\}, \quad (11)$$

where R is the gas constant $[J/mol \cdot K]$, P is the pressure $[bar]$, T is the temperature $[K]$, F is the surface generation rate, f is the mass fraction of mixture, φ_S is the mass fraction of soot.

The oxidation rate of soot also decides soot emission, according to chemical reaction kinetics and hybrid control theory of turbulence, S_{O_2} can be expressed by Nagle-Strickland·Constable Formula:

$$S_{O_2} = -F(\phi_S, P_{O_2}, T), \quad (12)$$

Then according to Magnussen-Hjertager formula, S_{O_2} can be expressed as:

$$S_{O_2} = -F(\phi_S, P_{O_2}, \tau), \quad (1)$$

where P_{O_2} is the partial pressure of O_2, T is the temperature $[K]$, τ is the time scale of turbulence integral.

3. The Establishment of the Mobile Grid

Using ESE module in FIRE software can automatically generate 1/4 combustion chamber shape in the grid interface after setting the grid parameters such as boundary layer and grid intensity, this is due to the selected 4 oil nozzles are arranged 360 degrees symmetrically. The combustion chambers corresponding to each nozzle can be considered as the same, so the combustion top dead point should be set to 720 degrees when generating grid. To simplify the design, only a part of the shape is visible. In the computing procedure, the grid will vary with the piston position, accurately simulate the piston movement, the combustion chamber model of meshing grid is shown in Fig. 1.

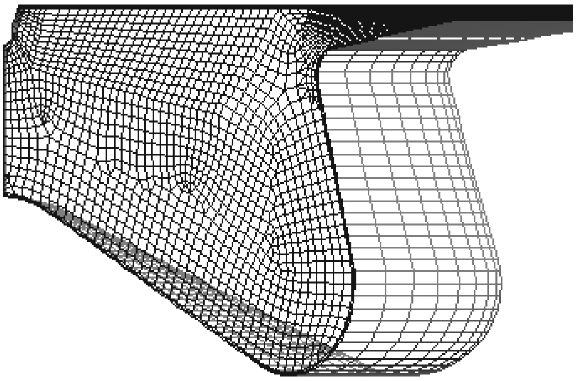

Fig. 1. The grid of combustion chamber/

4. The Analysis of Influence of Fuel Injection Advance Angle on Engine Combustion Procedure

4.1. The Simulation Analysis of Comparison of Combustion Process between Optimized Model and Original Machine Model

Fig. 2 has shown the comparison of accumulated heat release in cylinder between the original machine and optimized model. The accumulated heat release in cylinder of optimized model is about 14 % more than that of the original model. This demonstrates the improvement of optimized model performance.

Fig. 3 has shown the comparison of mean gas turbulence kinetic energy in cylinder between the original machine and optimized model. The mean gas turbulence kinetic energy of optimized model is about 2.7 % higher than that of the original model.

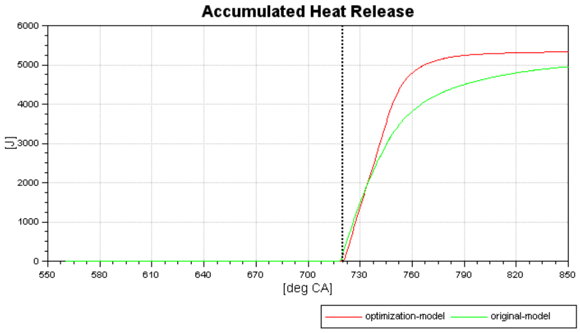

Fig. 2. Comparison of accumulated heat release.

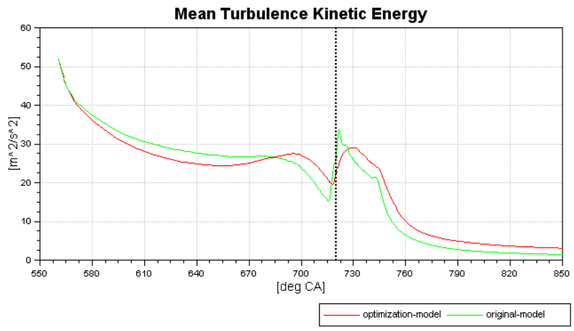

Fig. 3. Comparison of mean turbulence kinetic energy.

Fig. 4 has shown the comparison of mean temperature in cylinder between the original machine and optimized model. The mean temperature of optimized model is about 4.2 % higher than that of the original model.

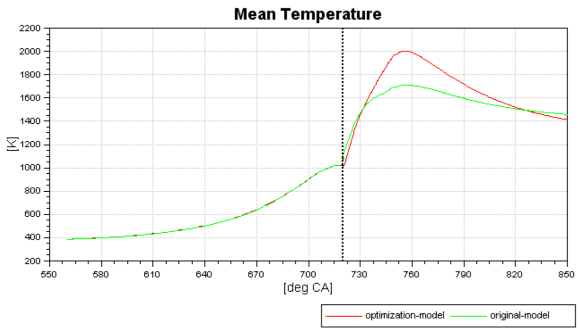

Fig. 4. Comparison of mean temperature.

Fig. 5 has shown the comparison of mean pressure in cylinder between the original machine and optimized model. The mean pressure of optimized model is about 4.8 % higher than that of the original model.

Fig. 6 has shown the comparison of mean NO mass fraction between the original machine and optimized model. The mean NO mass fraction of optimized model is slightly less than that of the original model. This demonstrates the improvement of NO_x emission of optimized model.

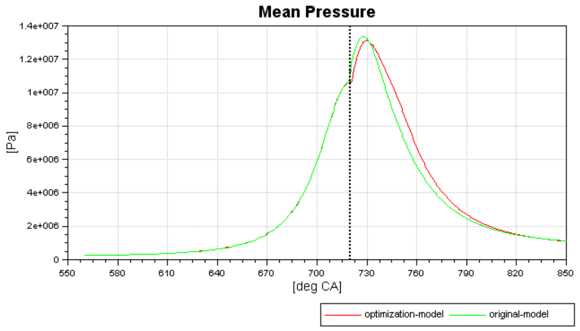

Fig. 5. Comparison of mean pressure.

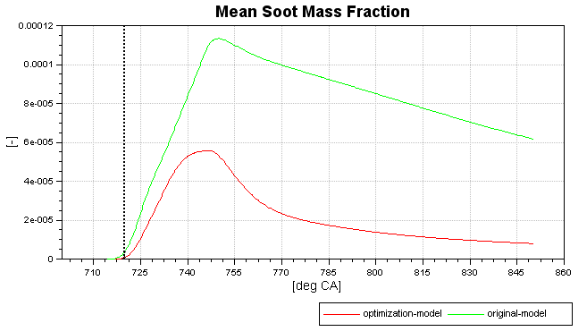

Fig. 7. Comparison of mean soot mass fraction.

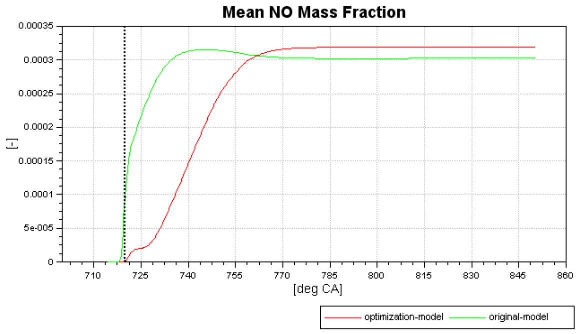

Fig. 6. Comparison of mean NO mass fraction.

Fig. 7 has shown the comparison of mean soot mass fraction between the original machine and optimized model. The mean soot mass fraction of optimized model is 30 % less than that of the original model. This demonstrates much improvement of NOx emission of optimized model.

4.2. The Simulation Analysis of Comparison of Temperature Field and Velocity Field between Optimized Model and Original Machine Model

4.2.1. Comparison and Analysis of Temperature Field

Fig. 8 shows the temperature field in cylinder of original model on the left, and that of optimized model on the right.

When reaching 20°CA before Top Dead Center, due to the same compression ratio, the temperature of 20°CA before the end of engine compression is essentially the same, because of no combustion, the distribution of temperature field in cylinder is relatively uniformed, and the average temperature in cylinder of both are very close.

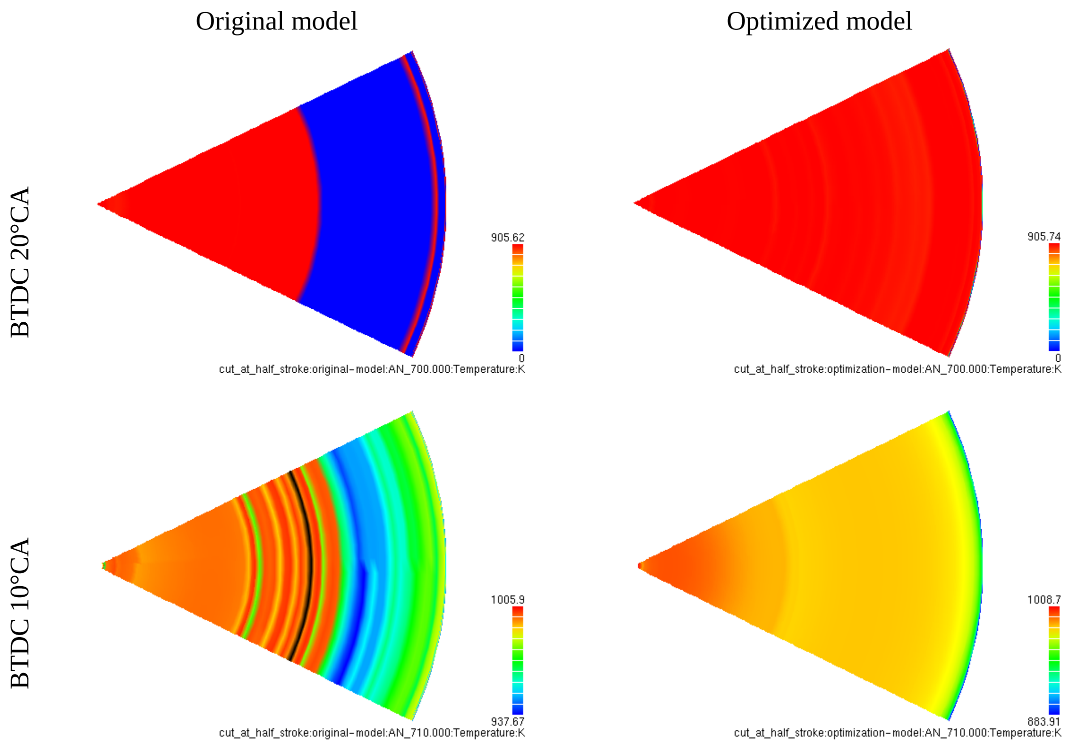

Fig. 8 (a). Comparison of temperature field in cylinder.

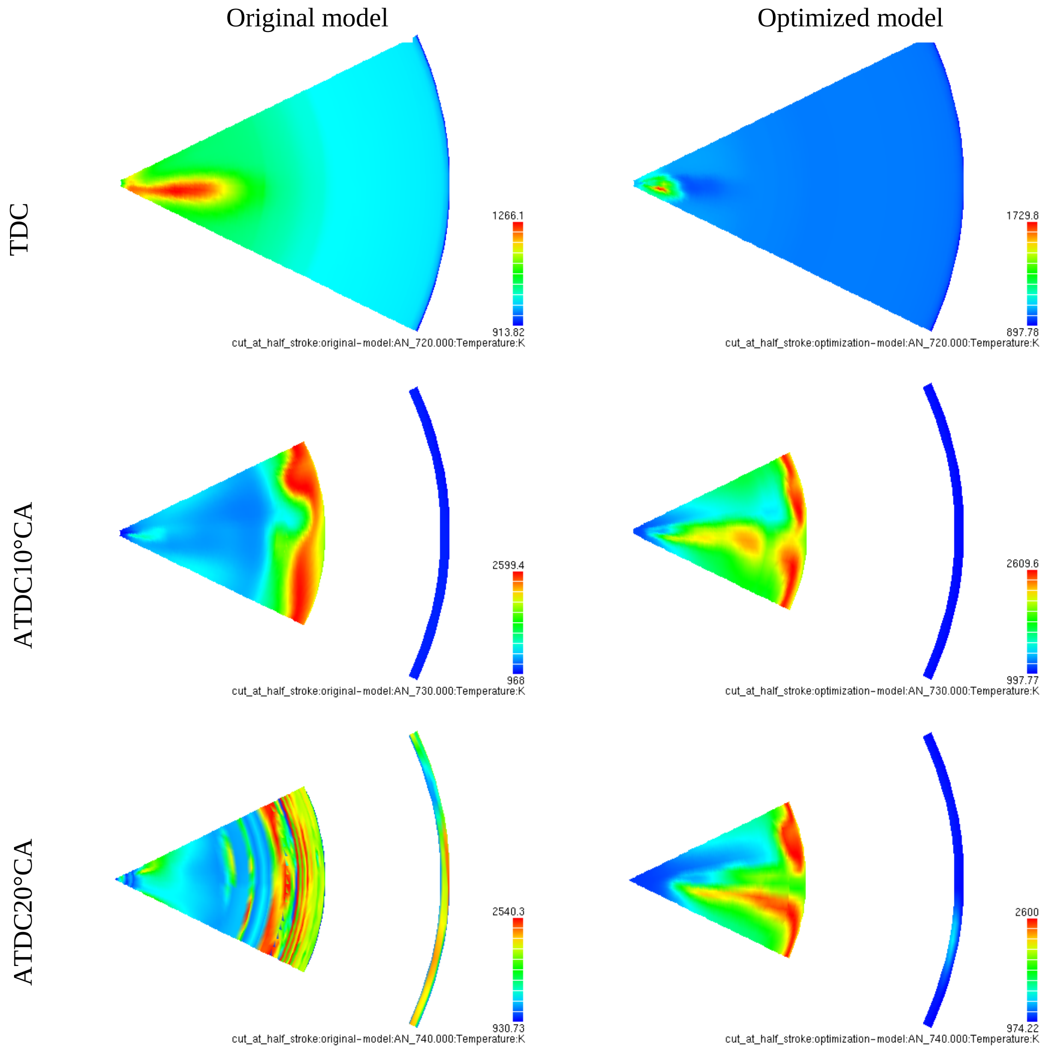

Fig. 8 (b). Comparison of temperature field in cylinder.

Continue compressing for 10°CA to reach 10°CA Before Top Dead Center, the temperature in cylinder rises, due to the same compression ratio, the temperature of 10°CA before the end of engine compression is essentially the same, because of no combustion, the distribution of temperature field in cylinder is relatively uniformed, and the average temperature in cylinder of both is very close.

Continue compressing for 10°CA to reach Before Top Dead Center, both engines have been injecting fuel, combustible mixture has been burning, the temperature of optimized model combustion chamber is higher, and the temperature of combusting area is up to 1729.6 K. The temperature of the original model combustion chamber is lower, and the temperature of combusting area reaches their highest 1266.1 K.

Crankshaft continues rotating for 10°CA to reach 10°CA after the Top Dead Center, combustible mixture of both have been burning more sufficiently, and both temperature in cylinder are very close, the temperature of optimized model combustion chamber is higher, and the temperature of the combusting area is up to 2609.6 K.

Crankshaft continues rotating for 10°CA to reach 20°CA After the Top Dead Center, namely 740°AC, both have finished burning combustible mixture essentially, the temperature dropped. Combustion temperature of optimized model is higher, and that of original model is lower. The combustion temperature field indicates that the temperature field in cylinder of optimized model is relatively higher.

4.2.2. Comparison and Analysis of Velocity Field

Fig. 9 shows the velocity field in cylinder of original model on the left, and that of optimized model on the right. When reaching 20°CA before Top Dead Center, Due to the different combustion chamber structures, the airflow velocity of 20°CA before the end of engine compression is different, the airflow velocity of original model combustion chamber is a bit higher.

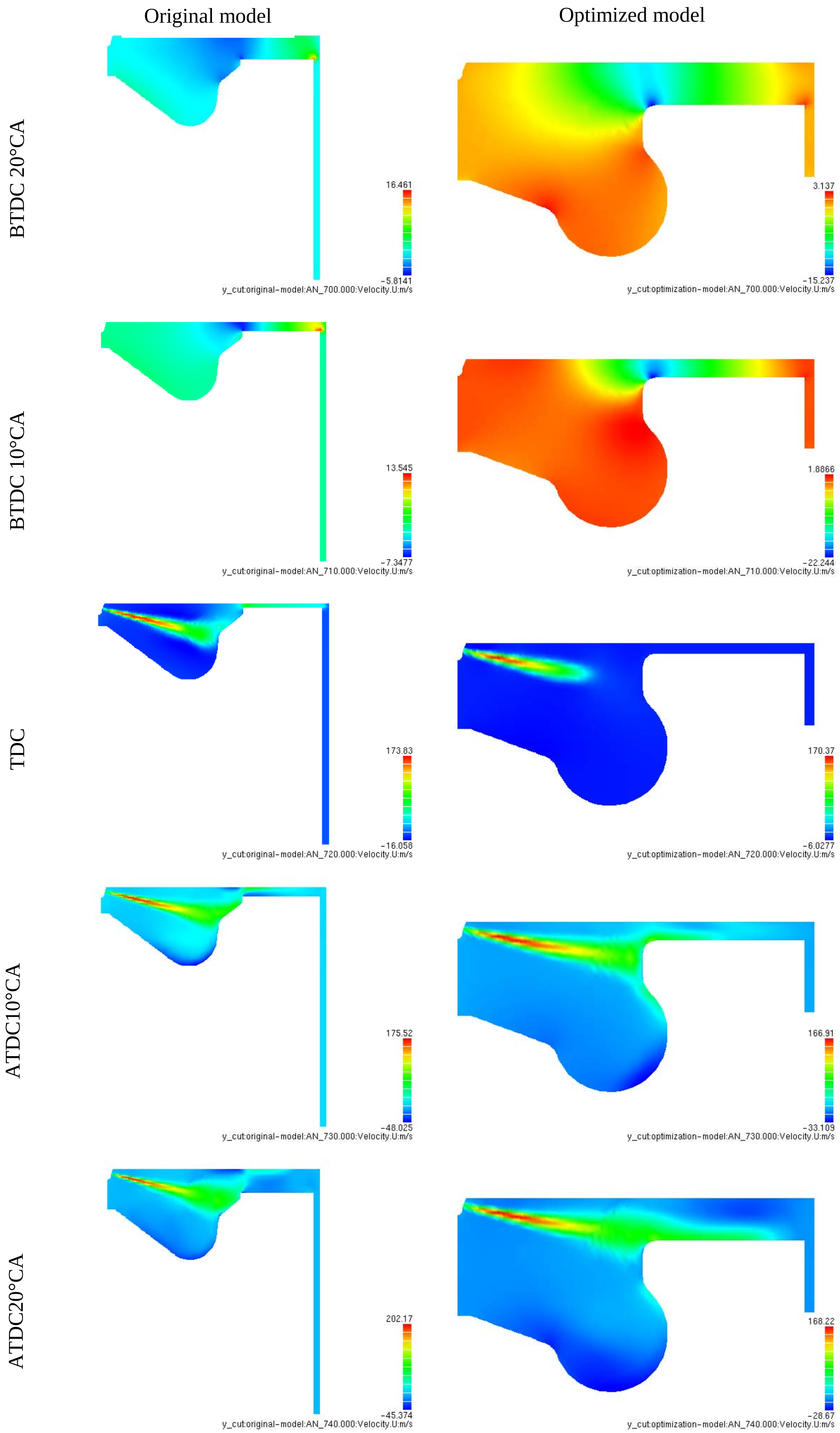

Fig. 9. Comparison of velocity field in cylinder.

Continue compressing for 10°CA to reach 10°CA before Top Dead Center, the airflow velocity in cylinder of both drop, because of no combustion, the distribution of velocity field in cylinder is relatively uniformed.

Continue compressing for 10°CA to reach Before Top Dead Center, both engines have been injecting fuel, combustible mixture has been burning, the combustion chamber airflow velocity of optimized model and C-type original model is similar.

Crankshaft continues rotating for 10°CA to reach 10°CA after the Top Dead Center, combustible mixture keeps burning, the combustion chamber airflow velocity of original model is higher.

Crankshaft continues rotating for 10°CA to reach 20°CA After the Top Dead Center, namely 740°AC, the airflow velocity in cylinder of both rise, the combustion chamber airflow velocity of original model is higher. The combustion velocity field indicates that airflow velocity of original model rises faster.

5. Experiment

This article is based on the modification of the original diesel engine, the main parameters of the original diesel engine are shown in Table 1.

Table 1. Basic technical data of diesel engine

Engine type	**Inline, water-cooled, four-stroke, double overhead camshaft**
Cylinder diameter X stroke	92×94
Emission(L)	2.499
Compression ratio	17.5
Intake valve open	15.6°(BTDC)
Intake valve close	64.4°(BTDC)
Exhaust valve open	66°(ATDC)
Exhaust valve close	32°(ATDC)
Rated power/ speed (kW/r/min)	105/4000
Maximum torque/speed (Nm/r/min)	340/2000
Minimum idling stabilized speed (r/min)	800
Cylinder work order	1-3-4-2
Exhaust gas temperature (°C)	< 650
Coolant temperature (°C)	< 85

Table 2 has shown the main test instruments and equipment used the optimized necking combustion chamber is adopted optimization combustion chamber. Other parameters are the same with the original machine.

Table 2. The main test instruments and equipment

No.	**Instrument Name**	**Type**	**Manufacturer**
1	Electric eddy current dynamometer	D160	Qidong Hongxing dynamometer factory
2	Exhaust gas temperature sensor	116E-6	Omega
3	Cylinder Pressure Sensor	6115BFD34A41	Kistler
4	Combustion analyzer	2893AK1	Kistler
5	The crankshaft angle adapter	2619A11	Kistler
6	Particle collection system	SPC 472	Kistler
7	Exhaust gas analyzer	FGA-41100	Fofen environmental protection testing equipment manufacturing co., LTD
8	Controller		self-design
9	Computer		assemble

5.1. Engine Performance Test

The previous sections have done a lot of design and calculation work about diesel engine combustion and emissions, and optimized fuel injection position. Fig. 10 has shown the performance curves of original machine and optimized engine. Test results show that the maximum torque of optimized engine declines about 6.4 %, and maximum power rises about 6.6 %, compared with the original machine.

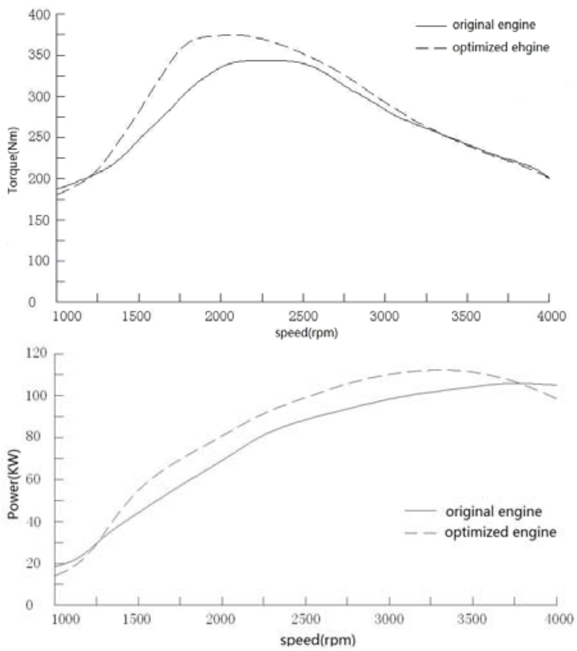

Fig. 10. Comparison of performance curves of original engine and optimized engine.

5.2. The Comparison of Engine Temperature and Pressure between Optimized and Original Engine

Fig. 11 shows the comparison of engine temperature between optimized and original engine. It indicates that the temperature of optimized engine is significantly higher than that of original engine. Fig. 12 shows the comparison of engine pressure between optimized and original engine. It indicates that the pressure of optimized engine is significantly higher than that of original engine.

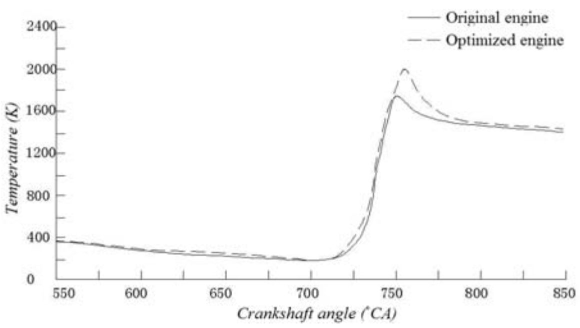

Fig. 11. Comparison of engine temperature between optimized and original engine.

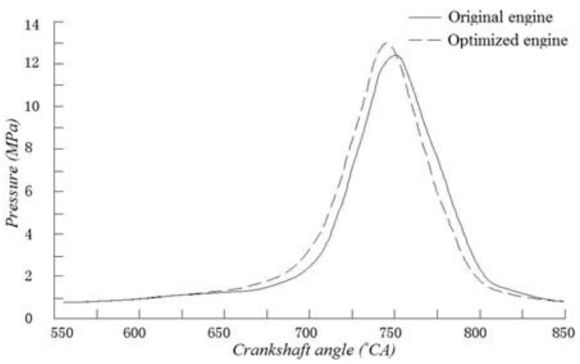

Fig. 12. Comparison of engine pressure between optimized and original engine.

5.3. ESC Test

To evaluate the purification effect of the optimized and original engine on NO_x and other exhaust pollutants, in accordance with the requirements of the test conditions, the ESC steady-state cycle test was carried on engine bench test before and after optimization. Fig. 13 shows the comparison of NO_x emission in the ESC engine cycle test before and after optimization. By optimizing the structure of engine to improve combustion effect, NO_x emission relatively decreased compared with original engine. Except idling procedure, in most of the working conditions, NO_x emission is 20 % less than that of original engine. Table 3 shows the emissions results of ESC steady-state cycle test. The results indicate that the ESC cycle test result is quite perfect, NO_x emission declined 3.6 %, and other emissions also decreased.

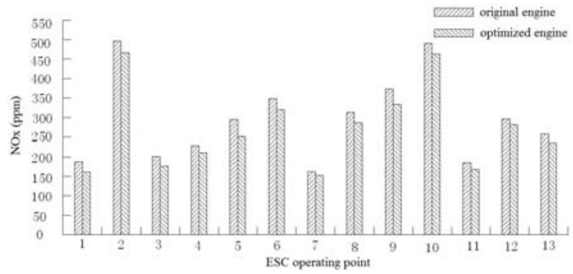

Fig. 13. NOx emission in the ESC engine cycle test.

Table 3. ESC test results.

Test Item	Original engine test values	Optimized engine test values	Deviation ratio
NOx[g/kWh]	3.36	3.24	decline 3.6 %
PM[g/kWh]	0.016	0.016	0
HC[g/kWh]	0.038	0.037	decline 2.6 %
CO[g/kWh]	0.13	0.13	0

5.4. ETC Test

ETC (European Transient Cycle) test is taken to measure the exhaust pollutants of diesel engine, it is the necessary means for testing diesel engine exhaust emissions. The ETC test pattern is shown in Fig. 14. Table 4 is the results of ETC steady-state test cycle emission. The test results indicate that the NO_x emission of original engine was 3.27 g/kWh, and 3.14 g/kWh after optimization, declined about 4 %, other emissions decreased in varying degrees.

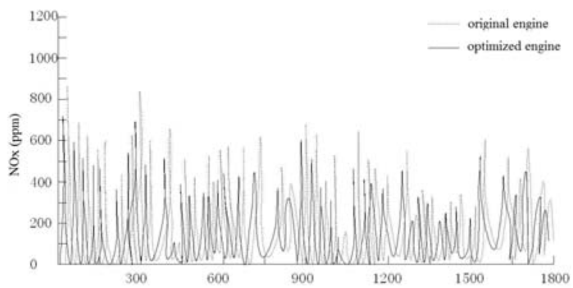

Fig. 14. ETC steady-state cycle test emission.

Table 4. ETC test result.

Test Item	Original engine test values	Optimized engine test values	Deviation ratio
NO_x[g/kWh]	3.27	3.14	decline 4 %
PM[g/kWh]	0.015	0.0149	decline 0.6 %
HC[g/kWh]	0.03	0.029	decline 3.3 %
CO[g/kWh]	0.12	0.118	decline 1.6 %

6. Conclusions

In the case of the optimization of diesel engine fuel injection advance angle, the influence on accumulated heat release in cylinder, mean turbulence kinetic energy of gas, NO_x and soot emission is simulated. Optimizing the structure is helpful to improve engine performance and reduce emissions. Finally with the Engine performance test, ESC and ETC emission test, the results are verified and indicate that the optimized structure can improve the diesel engine performance and reduce emissions, also put forward directional suggestions for design of diesel engine and research on performance experiment.

Acknowledgements

Project supported by the Shanghai University Experiment Technology Team Construction Project (No. E3-13SY14).

References

[1]. Rolf D. Reitz, Directions in internal combustion engine research, *Combustion and Flame*, Vol. 160, 2013, pp. 1-8.

[2]. Gao Song, Qu Jinyu, Present status of diesel emission regulation system and emission control technology development, *Journal of Shandong Institute of Technology*, Vol. 15, No. 3, September 2001, pp. 38-42 (in Chinese).

[3]. Zhu Hui, Wang Liqing, Zhang Youtong, Cheng Changqi, Dynamic simulation of diesel engine and control system using MATLAB/SIMULINK, *Transactions of CSICE*, Vol. 16, No. 3, 1998, pp. 314-321 (in Chinese).

[4]. R. Sausen, J. Hendricks, Impact of transport on climate, in *Proceedings of the 27th International Vienna Motor Symposium*, 27-28 April 2006.

[5]. He Kebin, Hao Jiming, Fu Lixin, Li Mingzhe, Liu Yang, The present situation and the development of automobile exhaust pollution of our country, *Environmental Science*, Vol. 17, No. 4, August 1996, pp. 80-83 (in Chinese).

[6]. Shen Yinggang, Wang Yulin, Zheng Wei, Shen Lizhong, Wei Jingsi, Combustion process numerical simulation technology development of internal combustion engine, *Tractor & Farm Transporter*, Vol. 1, 2004, pp. 7-9 (in Chinese).

[7]. Jiang Guodong, Zhu Gengshen, Feng Lizhu, Miao Shizhi, Ni Hanning, Numerical modeling and performance prediction of in-cylinder scavenging flow in a two-stroke uniflow type internal combustion engine, *Transactions of CSICE*, Vol. 8, No. 3, 1990, pp. 269-278 (in Chinese).

[8]. Du Aimin, Zhu Yanzhang, Jiang Sheli, Li Detao, Three-dimensional numerical simulation of the spray process in swirl chamber with a hybrid breakup model, *Transactions of CSICE*, Vol. 18, No. 1, 2000, pp. 24-28 (in Chinese).

[9]. Hu Jing, Zhao Yanguang, Chen Ting, Chen Zhen, Zhang Yunlong, Shuai Shijin,Wang Jianxin, Study of control strategy for Urea-SCR after-treatment system of heavy duty diesel engine, *Chinese Internal Combustion Engine Engineering*, Vol. 32, No. 2, April 2011, pp. 1-5 (in Chinese).

[10]. Zhang Guangde, Chen Zhi, Simulation and analysis for combustion of D. I. (Direct-Injection) diesel engines, *Internal Combustion Engines*, No. 1, February 2004, pp. 28-30 (in Chinese).

[11]. Ernst Estreit, Mathematical simulation of a large turbocharged two-stroke diesel engine, *Society of Automotive Engineers*, SAE Paper 710176.

[12]. O. L. Rackmil, A dynamical model of a locomotive diesel engine and electric hydraulic governor, *Journal of Engineering for Gas Turbines and Power*, 2005.

[13]. V. L. Krotov, Automatic control of internal combustion engine, *Mir Publisher*, Moscow, 2004.

[14]. Li Binxuan, Xu Hang, He Wenhua, Combution modeling for real-time simulation of diesel engine, *Transactions of CSICE*, Vol. 19, No. 2, 2001, pp. 148-152 (in Chinese).

[15]. A. P. Watkins, Flow and heat transfer in piston cylinder assemblies, Ph.D. Thesis, *University of London*, 1997.

[16]. A. D. Gosman, Y. Tsui and A. P. Wuins, Calculation of three dimensional air motion model engines, *Society of Automotive Engineers*, 1984, SAE paper 840299.

[17]. Liu Yongchang, The simulation of internal combustion engine thermal process, *China Machine Press*, Beijing, Vol. 2, No. 1, 2001, pp. 3-4.

[18]. J. K. Dukowicz, A partiele-fluid numerical model for liquid sprays, *Journal Computer Physics*, Vol. 35, No. 5, 1980, pp. 229-253.

[19]. Jiang Deming, The combustion and emissions of internal combustion engine, *Xi'an Jiaotong University Press*, Shanxi, 2002, pp. 24-52.

[20]. Li Xiaofen, Simulation study on combustion and emission process of high proportion of Dme-diesel mixed fuel, Master Thesis, *Taiyuan University of Technology*, 2010.

[21]. H. Hiroyasu, T. Kadota, Models for combustion and formation of nitric oxide soot in DI diesel engine, *Society of Automotive Engineers*, 1976, SAE Paper 760129.